International Journal of Medical Imaging
2020; 8(1): 6-15
http://www.sciencepublishinggroup.com/j/ijmi
doi: 10.11648/j.ijmi.20200801.12
ISSN: 2330-8303 (Print); ISSN: 2330-832X (Online)

Diffusion-Weighted Magnetic Resonance Imaging in Characterization of Neck Lymph Nodes in Head and Neck Cancer

Usama Elsaied Ghieda[1, *], Ahmed Abdul-Raheem Badr[2]

[1]Radiology Department, Faculty of Medicine, Tanta University, Tanta, Egypt

[2]Radiology Department, National Cancer Institute, Cairo University, Cairo, Egypt

Email address:
usama_ghieda@yahoo.com (U. E. Ghieda), dr.ahmed.a.badr@gmail.com (A. Abdul-Raheem B.)

[*]Corresponding author

To cite this article:
Usama Elsaied Ghieda, Ahmed Abdul-Raheem Badr. Diffusion-Weighted Magnetic Resonance Imaging in Characterization of Neck Lymph Nodes in Head and Neck Cancer. *International Journal of Medical Imaging.* Vol. 8, No. 1, 2020, pp. 6-15. doi: 10.11648/j.ijmi.20200801.12

Received: December 15, 2019; **Accepted**: December 30, 2019; **Published**: January 7, 2020

Abstract: Aim: to prospectively determine if diffusion weighted magnetic resonance imaging can help in discrimination between benign and malignant lymph nodes in patients with head and neck cancer, using histological results as the standard of reference. Patients & Methods: 40 patients complaining of palpable cervical lymph nodes with unknown primary malignancy or having known head and neck cancer. MRI neck study was done for all patients, including pre and post contrast sequences and DWI. Histopathology was done for all patients. Statistical analysis of the differences in ADC values for benign and malignant nodes was performed, together with further analysis of the differences between the ADC values of metastatic lymph nodes and lymphoma. Results: 30 patients were histopathological proved malignant lymphadenopathy (20 metastatic from head and neck malignancy and 10 primary lymphomas) and 10 patients were histopathological proved benign lymphadenopathy (1 acute reactive lymphadenitis, 1 chronic granulomatous inflammation, 4 chronic non-specific inflammation & 4 reactive lymphoid hyperplasia). A statistically significant difference between ADC values of benign and malignant cervical nodes was reported with a threshold ADC value equal to 1.30 $\times 10^{-3}$ mm2/sec was identified. The ADC value for lymphoma was less than that for metastatic carcinoma, with high specificity and sensitivity values and a threshold ADC value equal to 0.9 $\times 10^{-3}$ mm2/sec was identified. Conclusion: MR diffusion imaging is helpful non-invasive method in differentiation between benign and malignant lymph nodes, and to the same extent differentiation between the variant types of malignant lymphadenopathy.

Keywords: Diffusion-weighted Imaging (DWI), Apparent Diffusion Coefficient (ADC), Cervical Lymphadenopathy, Benign, Malignant, Reactive, Metastatic, Lymphoma

1. Introduction

The evaluation of cervical lymphadenopathy is important as they serve as an excellent clue to underlying problems. They could be due to infections, autoimmune disorders or malignancies (whether metastatic or lymphomas) [1].

Morphological imaging techniques such as US, CT & MRI allow the detection of enlarged cervical lymph nodes, yet none of these methods reaches the diagnosis. These imaging methods use standard parameters such as size, shape, internal architecture and pattern of enhancement [2-5]. Alternative imaging modalities such as SPECT and PET-CT could help to differentiate between benign and malignant lymph nodes, however these methods are expensive, time consuming and hampered by little spatial resolution [6].

The definitive method to differentiate benign and malignant lymph nodes is lymph node sampling, but biopsy methods are invasive and operator-dependent, with high incidence of false-negative results [7]. Therefore, there is an increasing need for noninvasive imaging techniques to help in discrimination between benign and malignant lymph nodes [8-10].

DWI is an MR technique that depicts molecular diffusion, which is the Brownian motion of water protons in biologic

tissues [11]. DWI performs with an EPI (echo planar imaging) sequence with linear regression after a logarithmic transformation of the signal intensity used to calculate the ADC values [12].

Many of the limitations regarding performance of extra-cranial DW imaging have recently been overcome, become easily performed with most standard 1.5- and 3-T clinical MR systems, and take only few minutes to obtain. Therefore, DW MR imaging has been increasing incorporated into wide variety of potential applications. Indications for DW imaging in the head and neck include characterization for primary tumors and nodal metastasis, monitoring of treatment response as well as differentiation of recurrent tumor from post therapeutic changes [13].

2. Aim of the Work

The aim of the study is to prospectively determine if diffusion weighted magnetic resonance imaging can help in discrimination between benign and malignant lymph nodes in patients with head and neck cancer, using histological results as the standard of reference.

3. Patients & Methods

Our Institutional Review Board approved this prospective study. An informed consent was obtained from all patients. The study was done on 40 patients referred to radiodiagnosis and imaging department of Tanta University Hospitals from January 2016 to July 2016. Patients were referred from the outpatient clinics complaining of palpable cervical lymph nodes with unknown primary malignancy (n=17) or having known head and neck cancer (n=23). MRI neck study was done for all patients, including pre and post contrast sequences and DWI. Histopathologic analysis was done for all patients [3 patients underwent excisional biopsy whilst 37 patients underwent fine needle aspiration cytology (FNAC)]. Patients with non-confirmed histopathological results were excluded from the study. No patients were excluded on basis of contraindication to MRI examination or history of contrast hypersensitivity.

3.1. MR Examination

3.1.1. Patient's Preparation

Patients with detachable metallic implant (teeth prosthesis) had to remove it prior to entrance to magnetic area. Fasting six hours before the MR scanning needed in 7 patients underwent anesthesia (6 patients suffered from claustrophobia and one uncooperative patient). Sedation was induced by ketamine sulphate (Ketalar) in a dose of 1-2 mg/kg slow IV.

3.1.2. MR Imaging Protocol

MR imaging examinations were performed with a 1.5-T MR imaging system (Signa EXCITE; GE Healthcare, Milwaukee, Wis). Patients were imaged in the supine position using a standard receive-only head and neck coil for both conventional imaging and diffusion-weighted MR imaging to include nodes from the base of the skull to the suprasternal notch. Axial and coronal T2- weighted with and without fat-suppression fast spin-echo sequences were initially performed, followed by axial T1-weighted with and without fat-suppression fast spin-echo sequences with parameters as shown on table 1.

A single- shot echo-planar DWI sequence was acquired using the parameters given in Table 1. The acquisition was performed using a maximum b value of 1000 s/mm^2. Pixel-wise ADC maps were generated by using a commercially available software workstation system (Advantage Workstation, version 4.2; GE Healthcare, Bue, France). Apparent diffusion coefficient (ADC) maps were calculated monoexponentially using the scanner software.

Gadoteric acid (DOTAREM®, Guerbet) was injected IV at a rate of 2 ml/s using a power injector, followed by a 20-ml saline flush. The dose of gadolinium was 0.1 mmol/kg of body weight for patients with normal renal function - that is, an estimated glomerular filtration rate (GFR) of more than 60 ml/min/1.73 m^2. No patients in this study had an estimated GFR of less than 60 ml/min/1.73 m^2. Post contrast T1-weighted imaging, with and without fat suppression was performed in the axial, coronal and sagittal planes.

Table 1. *MR Parameters.*

Parameter	T2- weighted imaging with and without with fat suppression	T1- weighted imaging with & without fat suppression	DWI	CE- T1- weighted imaging with and without with fat suppression
Repetition time (m.sec)	2500-4500	400-650	2000	740-775
Echo time (m.sec)	80	14	50–60	8-12
Flip angle (degrees)	90	90	90	15
Section thickness (mm)	5	5	5	5
Intersection gap (mm)	No	No	No	No
Matrix	320×224	256×192	256×256	288×224
Field of view (mm)	220	220	220	220
Voxel Size	RL 0.9, AP 1.1	RL 0.9, AP 1.1	RL 0.9, AP 1.1	RL 0.9, AP 1.1
No. of signals acquired	4	4	4	4

3.2. Imaging Analysis

The lymph nodes were characterized on the basis of internationally accepted standards for evaluating anatomic imaging data. At first, we detect the anatomical location of enlarged lymph nodes and describe them by the numerical grouping system. Then, the size and morphological features of lymph nodes as regard to their parenchymal homogeneity

and contrast enhancement were recorded.

The DW images and their corresponding ADC maps were analyzed in consensus at advantage workstation. The lymph nodes were localized on the images obtained with a b value of 0 sec/ mm^2. For quantitative assessment, multiple (2-3) regions of interest (ROI's) were placed over the lymph nodes identified on image with b value 0, on the basis of visual assessment and the software automatically copied these regions onto the other b value images. For non-necrotic lymph nodes, regions of interest were placed over the entire lymph node. While in necrotic lymph nodes, the regions of interest were placed over the solid components only. The smallest lymph node size for ADC calculation was 4mm in axial diameter to reduce the effects of partial volume artifacts. The mean ADC value of all used ROIs was denoted as the mean ADC for the lesion.

Finally, the radiologic findings were correlated with the histopathologic results, as the reference standard. The optimal ADC threshold with b values 0, 1000 for differentiating benign from malignant lymph nodes was determined by using receiver operating characteristic analysis. The sensitivity and specificity of the ADC values were subsequently calculated.

3.3. Statistical Analysis

Statistical analysis of the differences in ADC values for benign and malignant nodes was performed using one-way ANOVA test and Mann-Whitney U tests. Further analysis of the differences between the ADC values of metastatic LN and lymphoma was performed also using Mann-Whitney U test.

Receiver operating characteristic (ROC) curve analysis was done to test the ability of ADCs in differentiating benign and malignant lymphadenopathies and also primary (lymphoma) and secondary (metastases) malignant lymphadenopathies.

All statistical analyses were performed by using statistical software (Minitab 17, Minitab Inc., USA) and (Medcalc Software). $P < 0.05$ was considered to indicate a significant difference.

4. Results

This prospective study was conducted on 40 patients with cervical lymphadenopathy from January 2016 to July 2016; 21 males and 19 females, their ages ranged between 11-67 years (mean age 39.75±17.6 SD). According to histopathological results of our 40 patients; 10 patients were pathologically proven to be benign lymphadenopathy (1 acute reactive lymphadenitis, 1 chronic granulomatous inflammation, 4 chronic non-specific inflammation & 4 reactive lymphoid hyperplasia) and 30 malignant lymphadenopathy patients (20 metastatic from head and neck malignancy and 10 primary lymphomas).

The size of pathologically proven benign lymph nodes ranged between 1-3 cm (1.71±0.724) and the malignant nodes measured between 1.1-5.6 cm (2.54±0.92) there was statistically significant difference between the benign and malignant nodes as regard their size with p=0.0103. Morphological features of the benign and malignant LNs as regard to their numbers, borders, parenchymal homogeneity, enhancement pattern and presence of internal breakdown are shown in Table 2.

Table 2. *MR morphological features of the cervical lymphadenopathy of the patients in the study.*

Morphological Features		Benign lymph nodes	Malignant lymph nodes
Number of lymph node groups affected per patient	Single	3 (30%)	4 (3.33%)
	Multiple	7 (70%)	26 (86.67%)
Lymph Node Borders	Smooth	8 (80%)	15 (50%)
	Lobulated	2 (20%)	13 (43.33%)
	Speculated	0 (0%)	0 (0%)
	Indistinct	0 (0%)	2 (6.67%)
Enhancement	Weak	5 (50%)	11 (36.67%)
	Strong	5 (50%)	19 (63.33%)
Internal Breakdown	Present	2 (20%)	13 (43.33%)
	Absent	8 (80%)	17 (56.67%)

ADC Values

The ADC value for benign LNs ranged between 1.26×10^{-3} mm^2/s – 2.49 x $10^{-3}mm^2/s$ ($1.98 \pm 0.32\times10^{-3}$). The ADC value for malignant LNs ranged between $0.608\times10^{-3}mm^2/s$ – 2.1x $10^{-3}mm^2/s$ ($0.971 \pm 0.305\times10^{-3}$). There was a statistically significant difference between the benign and malignant nodes as regard their ADC values with $P<0.001$.

Further analysis of the ADC values in patients with metastatic LNs and Lymphoma showed that the ADC value for metastatic LNs ranged between $0.70\times10^{-3}mm^2/s$ – $2.10\times10^{-3}mm^2/s$ ($1.08 \pm 0.31\times10^{-3}$). The ADC value for lymphomatous LNs ranged between 0.608×10^{-3} mm^2/s – $1.16\times10^{-3}mm^2/s$ ($0.78 \pm 0.17\times10^{-3}$). There was a statistically significant difference between metastatic LNs and lymphoma as regard their ADC values with $P=0.0034$.

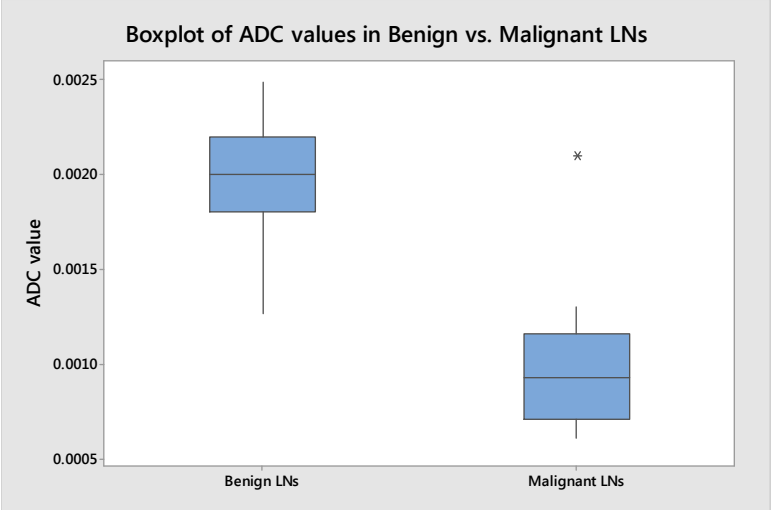

Figure 1. *ADC Values in Benign vs. Malignant LNs.*

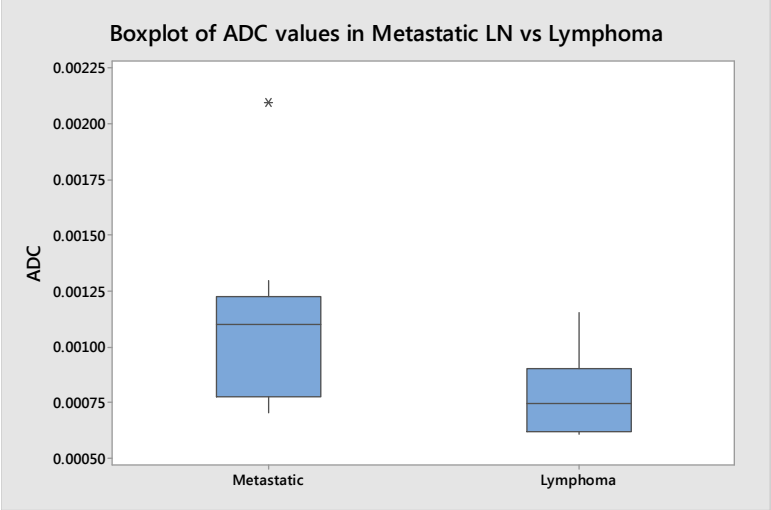

Figure 2. *ADC Values in Metastatic LNs vs. Lymphoma.*

One way ANOVA with interval plot for the ADC vaules of the three groups (benign vs. metastasis and lymphoma) showed statisicaly significnat difference between the ADC values of the different groups.

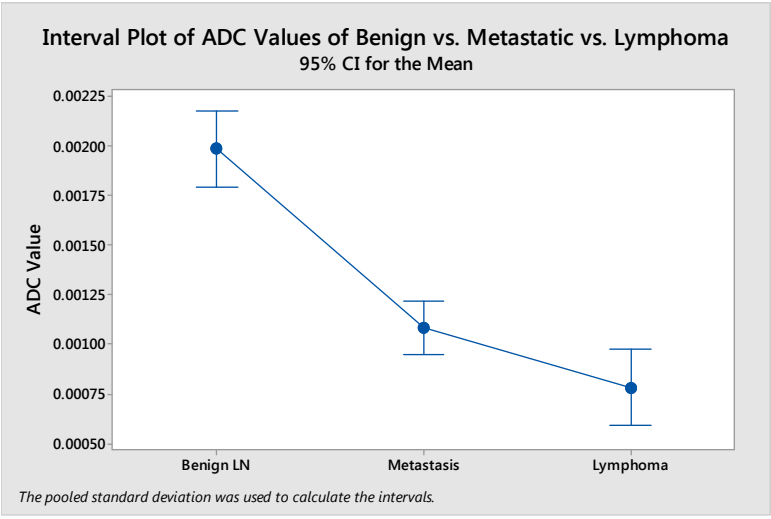

Figure 3. *ADC Values of Benign vs. Metastatic vs Lymphoma.*

The ROC curve analysis for ADC Values in benign vs malignant LNs revealed a sensitivity of 90.00% with 100% specificity for differentiation between the benign and malignant nodes for ADC Value ≤ 1.3×10^{-3} mm^2/s.

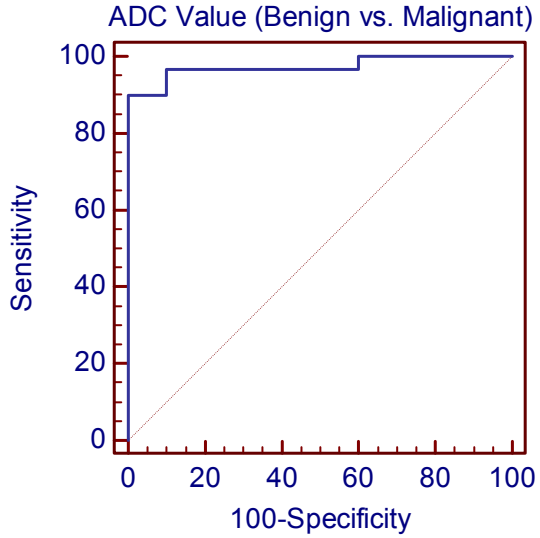

Figure 4. *ROC curve analysis for ADC Values in Benign vs. Malignant LNs.*

Further ROC curve analysis for ADC Values in Metastasis vs. Lymphoma revealed a sensitivity of 90.00% with 75% specificity for differentiation between the metastatic and lymphomatous nodes for ADC Value ≤ $0.9\times10^{-3}mm^2/s$.

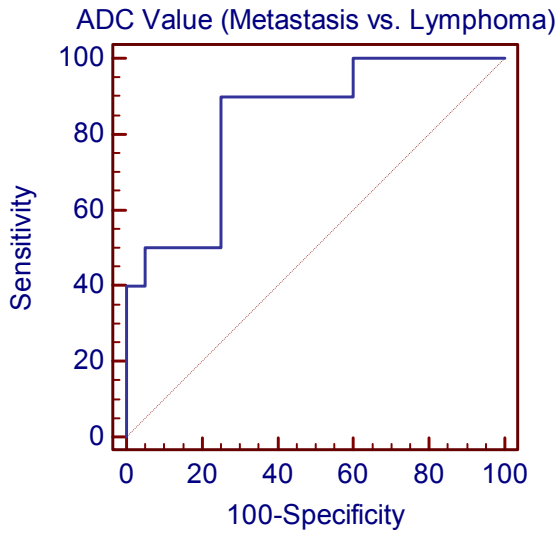

Figure 5. *ROC curve analysis for ADC Values in Metastasis vs. Lymphoma.*

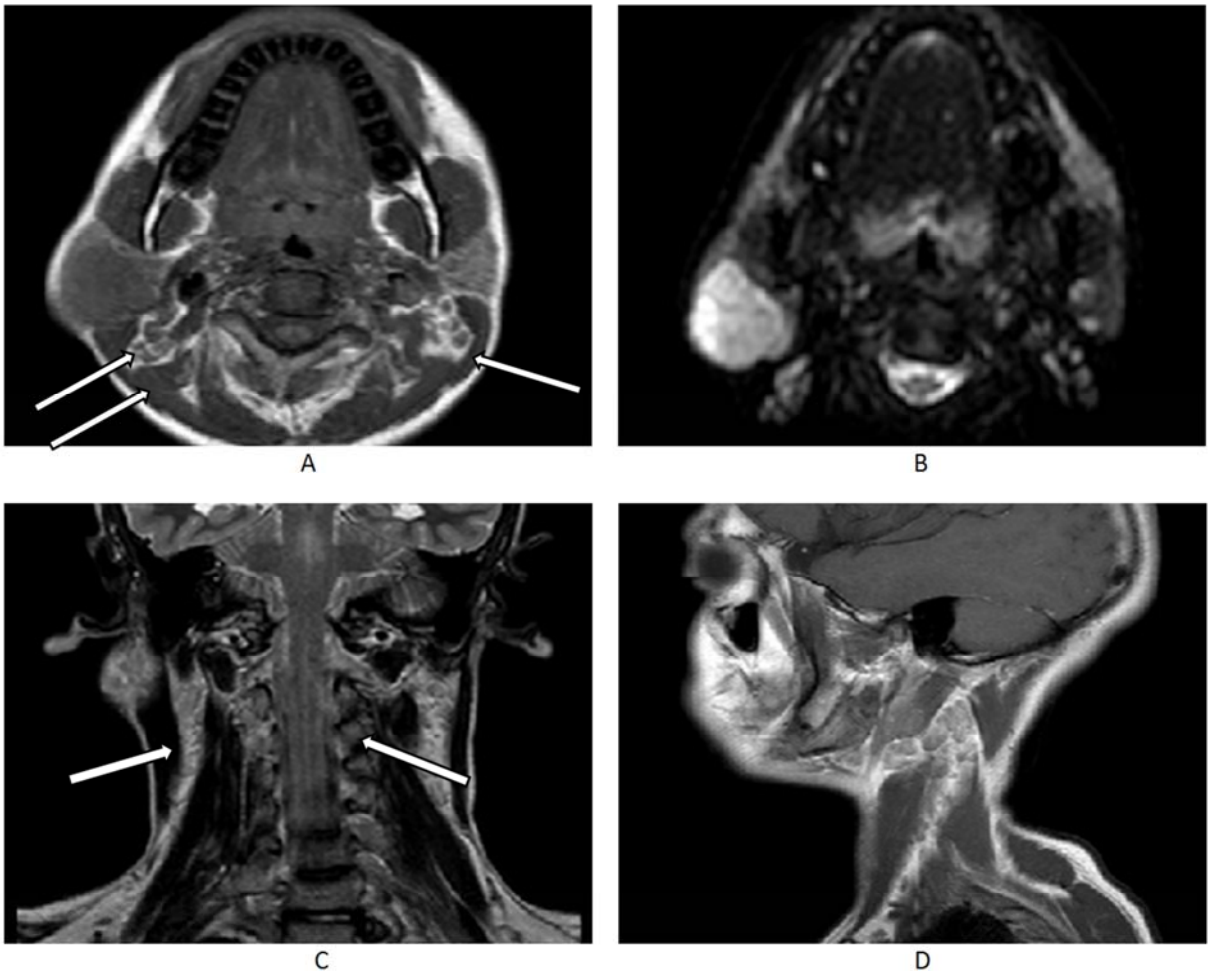

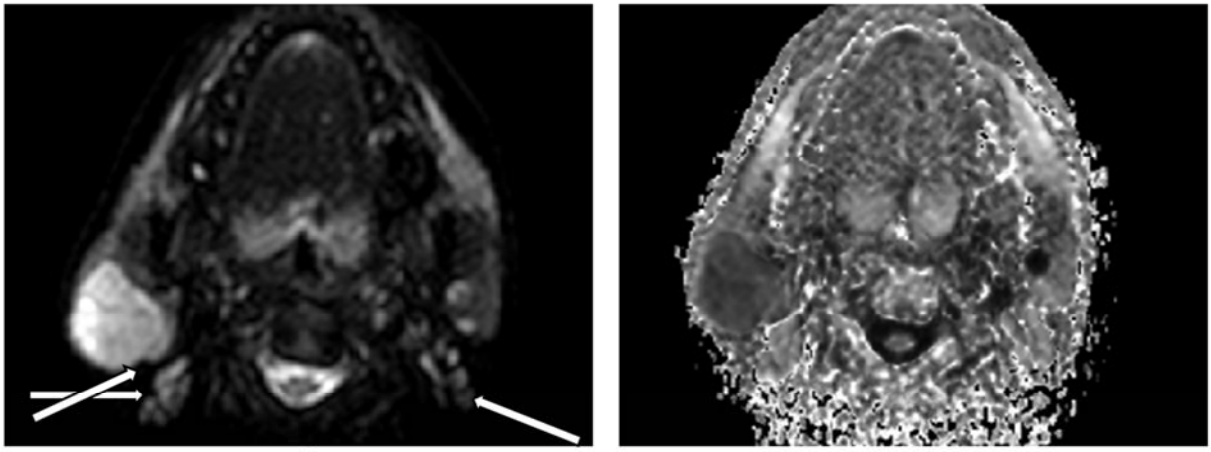

Figure 6. *30 years old male patient with right side upper neck swelling & bilateral upper deep cervical lymphadenopathy (groups II & III), largest measures 1.2cm in diameter.*

A: Axial T1 WI shows homogenous isointense right parotid mass lesion with bilateral isointense upper deep cervical lymph nodes.
B & C: Axial STIR & coronal T2 show mild heterogeneous hyperintense signals of the right parotid lesion with mild hyperintense signals of the cervical LNs.
D: Sagittal T1 post contrast shows fair contrast uptake of the cervical LNs, no remarkable areas of breaking down.
E & F: DWI (b 1000) & ADC map show restricted diffusion of the right parotid lesion with facilitated diffusion of the cervical LNs. Mean ADC values of the cervical LNs was $1.88\times10^{-3}mm^2/sec$.
Histopathological proved to be right parotid pleomorphic adenoma with benign cervical lymphadenopathy.

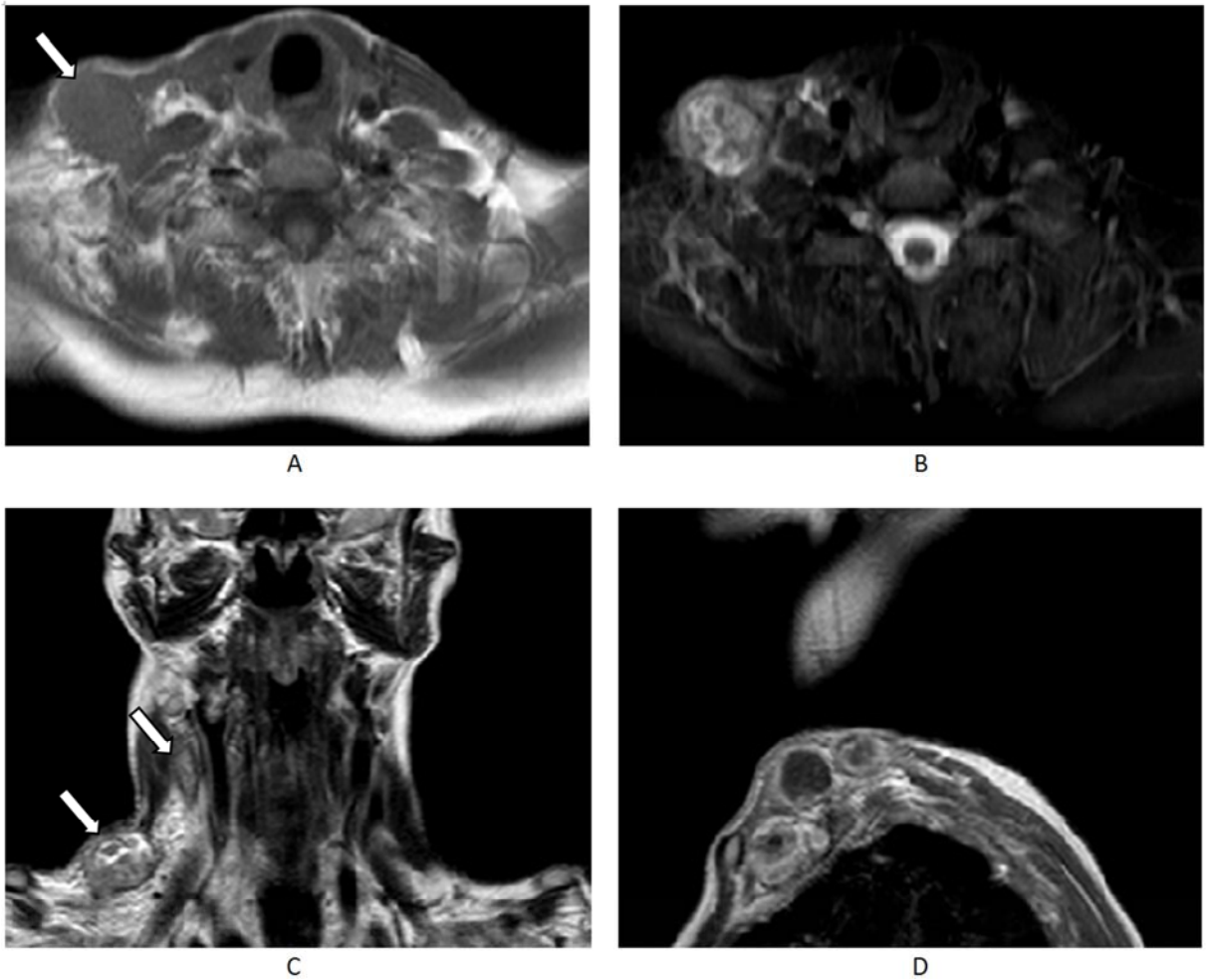

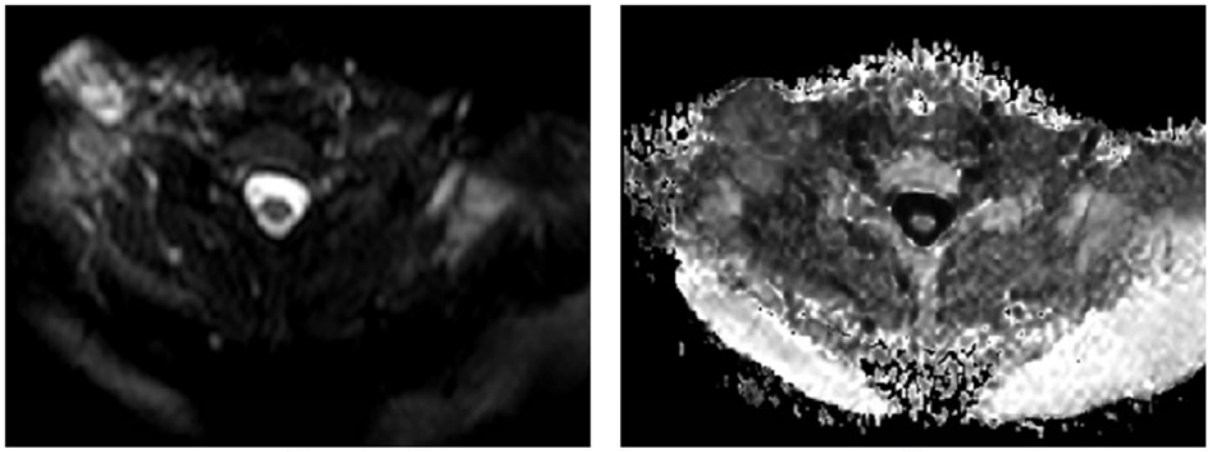

Figure 7. *40 years old male patient with right lower cervical lymphadenopathy groups II, III, V & right supraclavicular, largest measures 3.0 cm in diameter.*

A: Axial T1 WI shows homogenous isointense supraclavicular LN with regular border.
B & C: Axial STIR & coronal T2 show heterogeneous hyperintense signals.
D: Sagittal T1 post contrast shows fair contrast uptake with large area of breaking down.
E & F: DWI (b1000) & ADC map show restricted diffusion with low ADC value $0.983\times10^{-3}mm^2/sec$.
Histopathological proved to be metastatic lymphadenopathy from squamous cell carcinoma.

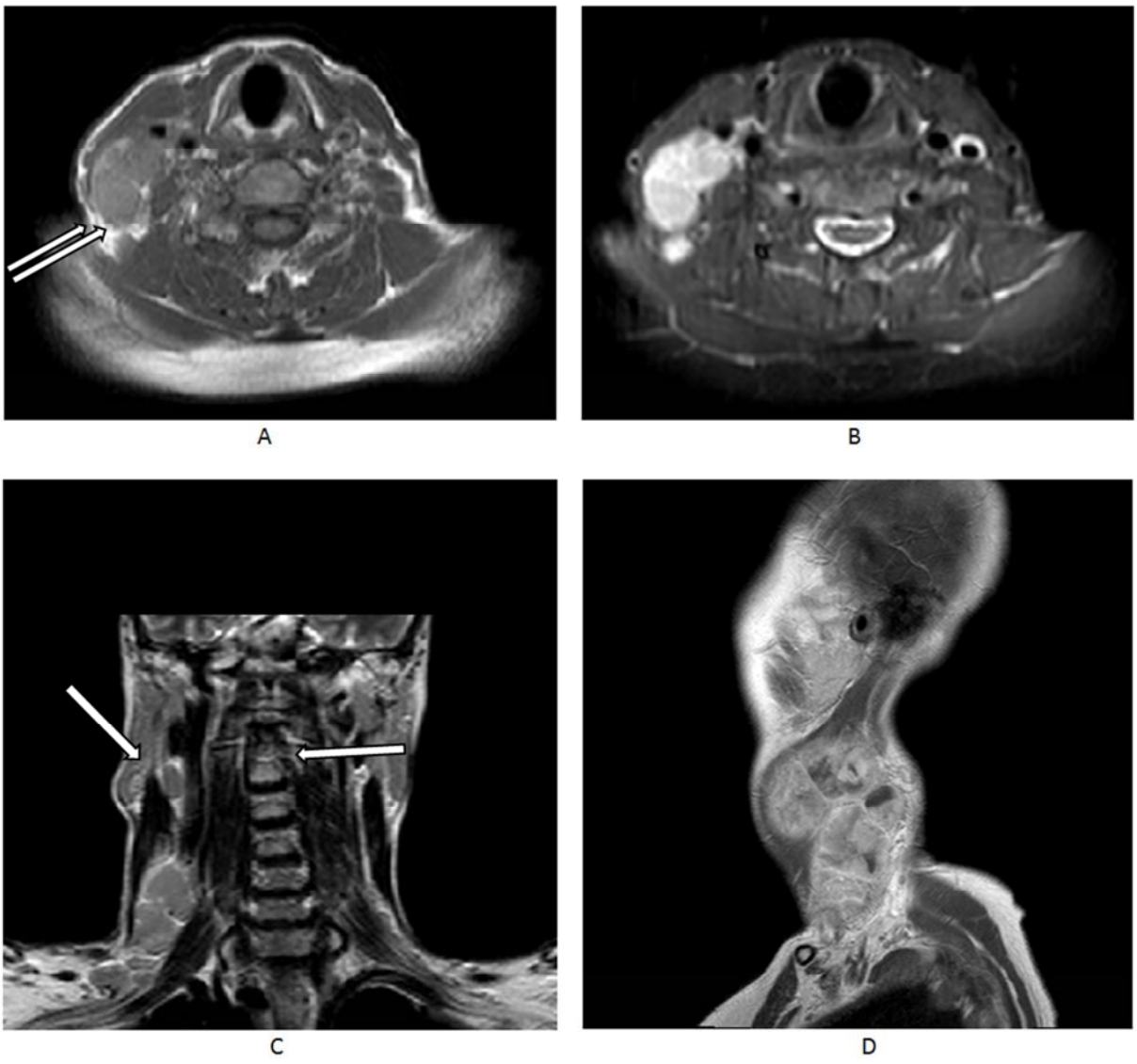

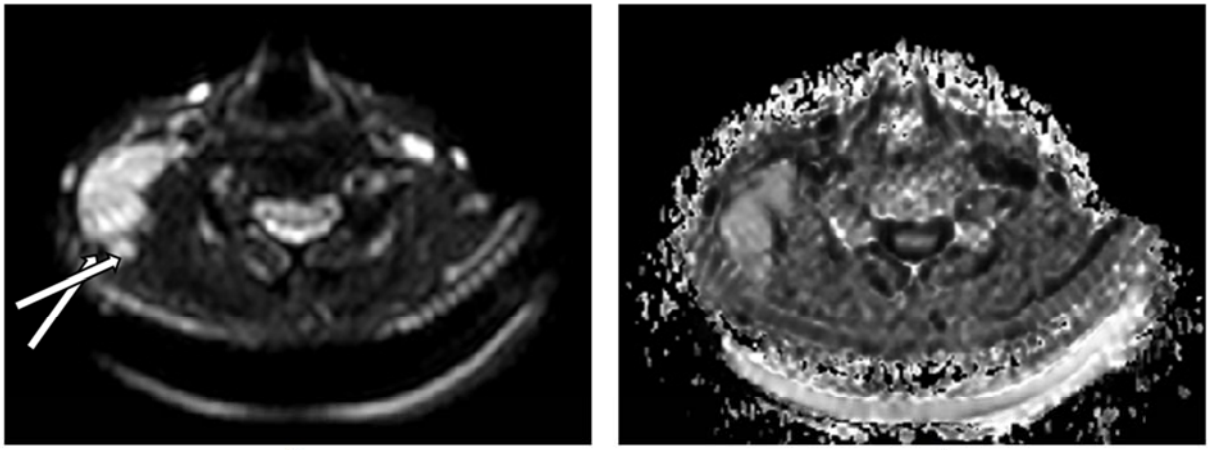

Figure 8. *57 years old male patient with right cervical lymphadenopathy groups II, III, IV& V, largest measures 3.0 cm in diameter.*

A: Axial T1 WI shows homogenous isointense LNs with smooth border.
B & C: Axial STIR & coronal T2 show heterogeneous hyperintense signals.
D: Sagittal T1 post contrast shows fair contrast uptake with areas of breaking down.
E & F: DWI (b1000) & ADC map show restricted diffusion with very low ADC value $0.791\times10^{-3}mm^2/sec$.
Histopathological proved to be Hodgkin's lymphoma (mixed cellularity).

5. Discussion

There is apparently increasing value to characterize head and neck lymphadenopathy as it helps in early detection of malignancies as well as determining the relevant line of treatment or management. The lymph nodes could be assessed by different radiological methods as US, CT and conventional MRI according to the following criteria: size, morphology and enhancement pattern which participate in suggesting the nature of the cervical lymph node whether it is benign or malignant [14, 15].

The lymph node is predicted to be benign if it is small in size (less than or equal 10 mm) and shows smooth lobulated borders as well as homogenous signal intensity of its parenchyma. Whilst predicted to be malignant if it is enlarged (more than 10 mm, especially when known primary cancer is present) or shows speculated, indistinct borders, and heterogeneous signal intensity of its parenchyma [14, 15].

Our study included 6 lymph nodes of diameter less than 1 cm with no morphological features of malignancy in conventional MRI, such as necrosis or indistinct margins; yet two of those six lymph nodes were proved to be metastatic. These results were in line with other studies [7, 16], stated that metastatic lymph nodes smaller than 1 cm could be missed owing to the size-based criteria for anatomic MR imaging, which may affect the clinical management in specific situations.

Diffusion gives good support or exclusion of the nature of the lymph nodes either being benign or malignant, depending upon on differences in water mobility. Malignant lymph nodes with hypercellular tissues will show restricted diffusion and low ADC values, while benign lymph node with low cellularity secondary to oedema or fibrosis will show facilitated diffusion and high ADC value [17, 18].

This study was conducted with high b value (1000 sec/mm^2) to overcome the effect of capillary perfusion and water diffusion in extracellular extravascular space, this will improve the specificity of the contrast on DWI. High b value also increase the relative contrast ratio between malignant and benign lesions & reduce signal-to-noise ratios. Pekçevik et al., 2015 [19], Vandecaveye et al., 2009 [20], Holzapfel et al., 2009 [6] & Perronea et al., 2011 [21] were using same b values in their studies.

In our study, all malignant nodes (n= 40) show restricted diffusion evidenced by increased signal on increasing the b-value (b= 1000) and low signal on ADC maps. These data are similar to studies carried by Perronea et al., 2011 [21] and Vandecaveye et al., 2009 [20].

We catch significant difference in ADC values of benign and malignant lymph nodes with P value <0.001. ADCs measurements of malignant lymph nodes were lower than those of benign lymph nodes. Furthermore, lymph nodes of lymphoma showed significantly lower ADCs values than those of metastatic lymph nodes with P value = 0.0034. These findings are in concordance with previous studies carried by Pekçevik et al., 2015 [19], Perronea et al., 2011 [21] & Sumi M. et al., 2006 [22] reported that the ADC values were significantly different among 3 node groups (metastatic, lymphoma and benign LNs).

In our study, the mean ADC value of the 30 malignant lymph nodes was $0.97\pm0.305\times10^{-3}mm^2/sec$ whereas the mean ADC value of the 10 benign lymph nodes was $1.98\pm0.33\times10^{-3}mm^2/sec$ with a threshold ADC value for differentiating malignant from benign nodes derived with receiver operating characteristic (ROC) analysis equals $1.30\times10^{-3}mm^2/s$ with sensitivity of 90% and a specificity of 100%. Abdel Razek AA et al., 2006 [23] reported slightly higher threshold (ADC: $1.38\times10^{-3}mm^2/s$) for reliably characterizing suspected lymph nodes with a sensitivity of 96% and specificity of 100%. Wang et al., 2001 [24] reported slightly lower threshold

(ADC: $1.22\times10^{-3}mm^2/s$) for distinguishing benign from malignant nodes, with a sensitivity of 91% and a specificity of 93%. Perronea et al., 2011 [21] reported lower threshold (ADC: $1.03\times10^{-3}mm^2/s$) for distinguishing benign from malignant nodes, with a sensitivity of 100% and a specificity of 92.9%.

Pekçevik et al., 2015 [19] reported a lower threshold (ADC: 1.02×10^{-3} mm^2/s) in characterizing metastatic lymph nodes with sensitivity of 94% and specificity of 100%. Their reported mean ADC values for benign and metastatic lymph nodes were $1.24 \pm 0.16 \times10^{-3}$ mm^2/s and $0.78 \pm 0.09 \times10^{-3}mm^2/s$ respectively. The relative difference in ADC values between our result and their results may be due to the fact that they calculated their ADC values using 3 different b-values. This explanation is supported by the findings of Vandecaveye et al., 2009 [20], who calculated the ADC values using 6 different b-values, described mean ADC values of $0.85\pm0.27\times10^{-3}$ mm^2 /s for metastatic lymph nodes versus $1.19 \pm 0.22 \times 10^{-3}$ mm^2/s for non-metastatic lymph nodes. Vandecaveye et al., 2009 [20] mean ADC values were lower compared those in the above cited reports. Thus, it is conceivable that the ADC curve shifts to the left when using DW-sequences with multiple b-values, where the influence of the signals derived from pseudo-diffusion is reduced.

Our study wasn't in agreement with Sumi M. et al., 2006 [22] who found – for metastatic nodes - significantly higher mean ADC value ($1.167\pm0.44\times10^{-3}$ mm^2/s) than benign lymphadenopathies ($0.652\pm0.10\times10^{-3}$ mm^2/s) and then lymphomatous ones ($0.601\pm0.427\times10^{-3}$ mm^2/s). This disagreement can be attributed to their use of low b values which worsen the sensitivity to diffusion, their selection of the region of interest on ADC maps, the use of sequences reduces artifacts to make more precise measurement for interested area as well as the large number of necrotic metastatic lymph nodes included in their study.

In our study, malignant lymph nodes were subdivided according to histopathology into subgroups: metastatic carcinoma and lymphoma. An attempt to differentiate between them on basis of their ADC values was done. The mean ADC value of metastatic carcinoma ($1.079\times10^{-3}mm^2/s$) was slightly higher (i.e., less restricted) than the ADC value of lymphoma ($0.781\times10^{-3}mm^2/s$) with a threshold ADC value for differentiating metastatic from malignant nodes derived with receiver operating characteristic (ROC) analysis equals $0.9\times10^{-3}mm^2/s$ with sensitivity of 90% and a specificity of 75%. The differences in degree of diffusion restriction may be attributed to greater cellularity and less extracellular space in lymphoma than metastatic carcinoma. These data were in line with King AD et al., 2007 [7], who reported significant differences among ADC values of metastatic nodes of differentiated squamous cell carcinoma (SCC), undifferentiated carcinoma and lymphoma, with the ADC value for SCC ($1.057\times10^{-3}mm^2/s$) was greater than that for undifferentiated carcinoma ($0.802\times10^{-3}mm^2/s$) and that for lymphoma ($0.664\times10^{-3}mm^2/s$); they reported ADC value of less than $0.767\times10^{-3}mm^2/s$ could be used to distinguish lymphoma, with a specificity of 100% and a sensitivity of 88%.

Statistical data obtained in our study were 34 true-positive, 6 false-positive findings, yielding 100% sensitivity, and 85% specificity. False decrease in ADC value in benign lymph nodes could be attributed to benign nodal reactive changes like multiple germinal centers and fibrotic stroma acting as microstructural barriers as described by Wang J et al., 2001 [24]. Vandecaveye et al., 2009 [20] described lower specificity of DW imaging with false decrease in ADC secondary to nodal reactive changes & subsequent overestimation of the metastatic burden, thus suggested combined use of DW imaging and anatomic features indicative of benignity to the false-positive rate. Choi KD et al., 2007 [25] also stated false-positive readings with restricted diffusion secondary to recent hemorrhage and suggested to avoid DW imaging shortly after biopsy.

Our study had limits of being a small study cohort with no other major limitation could be detected to greatly affect the study results.

6. Conclusion

MR diffusion imaging is helpful non-invasive method in differentiation between benign and malignant lymph nodes, and to the same extent differentiation between the variant types of malignant lymphadenopathy.

References

[1] Sambandan T, Christefi Mapel R. Review of cervical lymphadenopathy. JIADS 2011; 2: 31-33.

[2] Curtin HD, Ishwaran H, Mancouso AA, Dalley RW, Caudry DJ, McNeil BJ. Comparison of CT and MR imaging in staging of neck metastasis. Radiology 1998; 207: 123–130.

[3] Castelijns JA, van den Brekel MW. Imaging of lymphadenopathy in the neck. Eur Radiol 2002; 12: 727–738.

[4] Kaji A, Mohuchy T, Swartz JD. Imaging of cervical lymphadenopathy. Semin Ultrasound CT MR 1997; 18: 220–249.

[5] Fischbein N, Noworolski S, Herny R, Kaplan M, Dillon W, Nelson S. Assessment of metastatic cervical adenopathy using dynamic contrast-enhanced MR imaging. AJNR Am J Neuroradiol 2003; 24: 301–311.

[6] Holzapfel K, Duetsch S, Fauser C, et al. Value of diffusion-weighted MR imaging in the differentiation between benign and malignant cervical lymph nodes. Eur J Radiol 2009; volume 72 (3): 381–7.

[7] King AD, Ahuja AT, Yeung DK, et al. Malignant cervical lymphadenopathy: diagnostic accuracy of diffusion-weighted MR imaging. Radiology 2007; 245: 806–813.

[8] Jakobsen J, Hansen O, Jorgensen E, and Bastholt L. Lymph node metastasis from laryngeal and pharyngeal carcinomas-calculation of burden of metastasis and its impact on prognosis. Acta Oncologica 1998; 37: 489-575.

[9] Kehrl W, Wenzel S, Niendorf A. Effect of various form of metastatic lymph node involvement om prognosis of squamous epithelial carcinomas of the upper aerodigestive tract. Laryngo-Rhino-Otolgie, 1998; 77: 569-575.

[10] Leemans CR, Tiwari R, Nauta J, Van Der Waal I and Snow GB. Recurrence at the primary site in head and neck cancer and the significance of neck lymph node metastasis as a prognostic factor.

[11] Thoeny HC, De Keyzer F, Claus FG, Sunaert S, Hermans R. Gustatory stimulation changes the apparent diffusion coefficient of salivary glands: initial experience. Radiology 2005; 235 (2): 629–634.

[12] Thoeny HC, De Keyzer F. Extracranial applications of diffusion weighted MR imaging. Eur Radiol 2007; 245: 806-813.

[13] Thoeny HC, De Keyzer F, King AD, Diffusion weighted MR imaging of head and neck, Radiology 2012; 263: 19-32.

[14] Grégorie, V, Lefebvre JL, Licitra F, Felip E. Squamous cell carcinoma of the head and neck: Clinical practice guidelines for diagnosis, treatment and follow-up. Ann. Oncol. 2010; 21: 184-186.

[15] Barchetti F, Pranno N, Giraldi G, et al. Role of 3 tesla diffusion-weighted imaging in the differential diagnosis of benign versus malignant cervical lymph nodes in patients with head and neck squamous cell carcinoma, BioMed Research International 2014, Article ID 532095, 9 pages.

[16] Van den Brekel MW. Lymph node metastases: CT and MRI. Eur J Radiol 2000; 33: 230–238.

[17] Takahara T, Imai Y, Yamashita T, et al. Diffusion weighted whole body imaging with background body signal suppression (DWIBS): technical improvement using free breathing, STIR and high resolution 3D display. Radiat Med 2004; 22: 275–282.

[18] Koh DM and Collins DJ. Diffusion-weighted MRI in the body: applications and challenges in oncology. AJR Am J Roentgenol 2007; volume 188: number 6, pages 1622–1635.

[19] Pekçevik Y, Çukurova I, Arslan IB. Apparent diffusion coefficient for discriminating metastatic lymph nodes in patients with squamous cell carcinoma of the head and neck. Diagn Interv Radiol 2015; 21: 397–402.

[20] Vandecaveye V, De Keyzer F, Vander Poorten V, et al. Head and neck squamous cell carcinoma: value of diffusion-weighted MR imaging for nodal staging. Radiology 2009; volume 251, number (1): pages 134–146.

[21] Perronea A, Guerrisia P, Izzob L, D'Angelic I, Sassi S, Melea LL, Marinia M, Mazzaa D, Marinia M. Diffusion-weighted MRI in cervical lymph nodes: Differentiation between benign and malignant lesions, European Journal of Radiology 2011; 77: 281–286.

[22] Sumi M, Van Cauteren M, Nakamura T, et al. MR micro-imaging of benign and malignant nodes in the neck. AJR American journal of Roentgen -ology 2006; volume 186: pages 749–757.

[23] Abdel Razek AA, Soliman NY, Elkhamary S et al. Role of diffusion-weighted MR imaging in cervical lymphadenopathy. Eur Radiol 2006; volume 16: pages 1468-77.

[24] Wang J, Takashima S, Kawakami F, et al. Head and neck lesions: characterization with diffusion-weighted echo-planar MR imaging. Radiology 2001; volume 220: pages 621–630.

[25] Choi KD, Jo JW, Park KP, et al, Diffusion weighted imaging of intramural hematoma in vertebral artery dissection. J Neurol Sci, 2007; volume 253: pages 81–84.